ELSEVIER

Ceramics International 30 (2004) 1141–1146

CERAMICS INTERNATIONAL

www.elsevier.com/locate/ceramint

Study of 1-3 composite transducer for ultrasonic wirebonding application

C.P. Chong [a,b], H.L. Li [a,b], H.L.W. Chan [a,*], P.C.K. Liu [b]

[a] *Department of Applied Physics and Materials Research Centre, The Hong Kong Polytechnic University, Hunghom, Kowloon, Hong Kong, China*
[b] *ASM Assembly Automation Ltd., 12/F, Watson Centre, 16 Kung Yip St., Kwai Chung, Hong Kong, China*

Received 26 November 2003; accepted 18 December 2003

Available online 5 June 2004

Abstract

Lead zirconate titanate (PZT)/epoxy 1-3 composites consisted of PZT rods embedded in an epoxy matrix were used as the driving elements in an ultrasonic wirebonding transducer for microelectronic packaging. The performance of the 1-3 composite PZT transducer with 0.91 volume fraction of PZT has been studied. The composite transducer has fewer lateral vibrations and higher damping. It has the potential to be used in new generation high-speed and fine-pitch ultrasonic wirebonding machines.

Keywords: D. Lead zirconate titanate (PZT); 1-3 Composite; Ultrasonic wirebonding transducer

1. Introduction

Combining piezoelectric ceramics with a passive polymer phase can form a variety of new piezoelectric materials. 1-3 Composites [1–6] consisting of piezoceramic rods embedded in a polymer matrix have attracted considerable attention because of their uses in medical ultrasound and underwater acoustic transducers. By proper selection of the ceramics, polymer, volume fractions, and aspect ratio of the ceramic element (width to height ratio, L/T), the composite properties can be tailored to meet specific device requirements. The resonance characteristics and mode coupling of 1-3 composites have been widely studied [1–6]. Ring-shaped lead zirconate titanate (PZT) ceramics have been used extensively as the driving elements in ultrasonic wirebonding transducers. In a wirebonding transducer, as the length of the driver (a Langevin sandwich transducer) is comparable to the diameter of the ring, therefore, the radial and wall-thickness resonances of the ring may couple with the desired axial mode of the transducer [7–10]. Moreover, PZT has a high mechanical quality factor Q_m and hence it has a very sharp resonance with limited bandwidth and causes frequency tuning and locking problems in the bonding machine. To alleviate these problems, 1-3 composite rings have been used to suppress mode coupling and maintain a pure axial mode [7–9].

In this study, PZT/epoxy 1-3 composite rings with PZT volume fractions ϕ ranging from 0.58 to 0.93 have been fabricated. A composite transducer using four $\phi = 0.91$ composite rings have been assembled. A commercial FEM code was used to analyze the vibration characteristics of the composite transducers and compared to experimental results. A PZT transducer of similar structure has also been fabricated and its performance compared to that of the composite transducer.

2. Samples preparation

1-3 Composite rings were fabricated by the dice-and-fill technique [7,8]. Commercial PZT8 rings (12.7 mm o.d., 5.05 mm i.d., and 2.3 mm thickness) supplied by ASM were used. Araldite LY5138-2/HY5138 epoxy was used as the passive phase. Parallel grooves were cut in two perpendicular directions on the PZT rings using a Disco DAD 321 automatic dicing saw equipped with a 75 μm thick diamond saw blade. Due to blade vibration, the resulting grooves were about 77–81 μm in width. By making different number of cuts per direction from 5 to 39, composite rings with

* Corresponding author. Fax: +86-852-2333-7269.
E-mail address: apahlcha@polyu.edu.hk (H.L.W. Chan).

0272-8842/$30.00
doi:10.1016/j.ceramint.2003.12.013

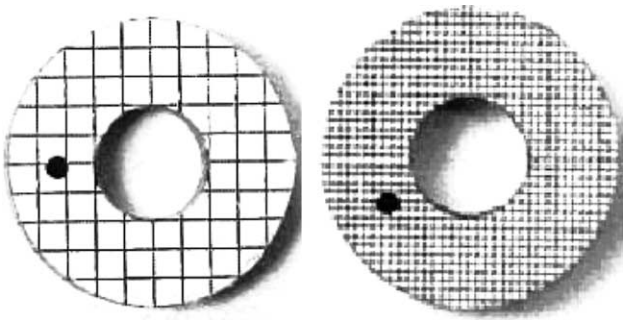

Fig. 1. Photographs showing 1-3 composite rings with two different ceramic volume fractions ϕ (a) 0.88, (b) 0.63.

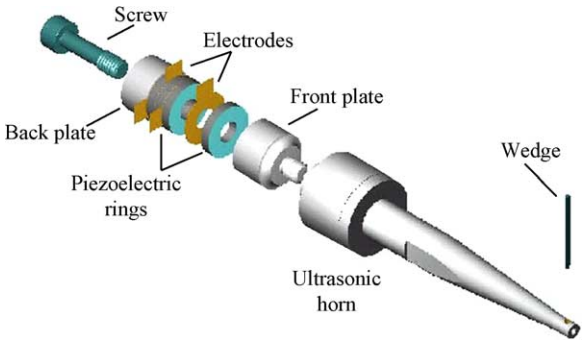

Fig. 2. Assembly diagram of the bonding transducer with piezocomposite rings.

different PZT element widths and different ceramic volume fraction ϕ ranging from 0.93 to 0.58 were obtained. Epoxy was then filled into the grooves under vacuum, and after the epoxy has cured, the composite rings were polished and air-dried silver paint was applied to the two flat surfaces as electrodes. The samples with $\phi = 0.88$ and 0.58 are shown in Fig. 1.

Descriptions of the composite rings are tabulated in Table 1. The composite rings have sufficiently small epoxy width (~78–81 μm) and can be treated as a homogenous material with a set of effective material properties. An ultrasonic wirebonding transducer operated at ~64 kHz is schematically shown in Fig. 2. It consists of three main parts, namely, the driver, amplifying horn, and the wedge. Each transducer consists of four composite (or PZT) rings. The four rings are connected electrically in parallel and mechanically in series and sandwiched between the front

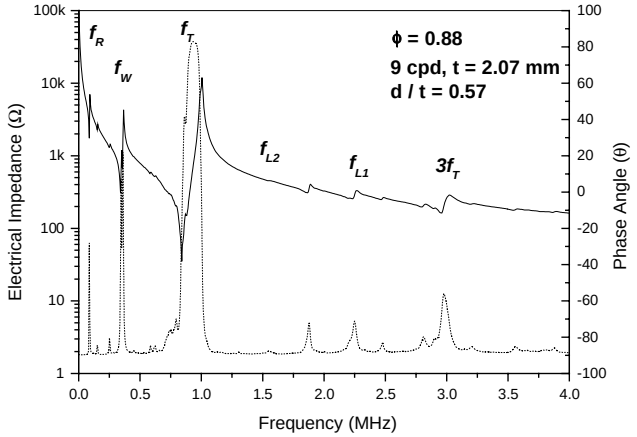

Fig. 3. Plots of electrical impedance (solid line) and phase angle (dot line) vs. frequency for a $\phi = 0.88$ composite ring.

and back metal plates by a pre-stressed screw. The composite rings used in the present study have $\phi = 0.91$ (with 7 cuts per direction, cpd). This is a compromise between cost and performance, as more cuts per direction will increase the cost of fabrication. It has been found that composite rings with $\phi = 0.91$ have adequate performance. Another wirebonding transducer with similar structure using PZT8 rings as the driving elements has also been fabricated and the performance of the ceramic and composite transducers were evaluated and compared.

3. Resonance modes in 1-3 composite rings

The ceramic and composite rings were poled in the thickness direction and the electrical impedance and phase spectra of the rings were measured using an HP4194A impedance analyzer. Resonance modes of a 1-3 piezocomposite ring can be classified into two main categories (Fig. 3) as follows [4–6]:

1. Characteristic resonances of individual PZT elements inside the ring which include:
   (a) The thickness mode resonance f_T; and
   (b) The coupled lateral mode resonances f_{L1} and f_{L2}.
2. Cooperative resonances of the whole ring:
   (a) The radial (f_R) and wall-thickness (f_W) mode resonances; and

Table 1
1-3 Piezocomposite rings with 12.7 mm o.d., 5.05 mm i.d., and ~77–81 μm epoxy width

Type	PZT8	PZT8/Epoxy 1-3 composite									
Cuts per direction (cpd)	0	5	7	9	13	17	21	25	29	33	39
PZT volume fraction, ϕ	1.0	0.93	0.91	0.88	0.84	0.79	0.75	0.71	0.67	0.63	0.58
PZT element aspect ratio (L/T)	–	0.99	0.75	0.57	0.47	0.38	0.32	0.28	0.25	0.18	0.15
Average thickness (mm)	2.30	2.05	2.0	2.07	1.94	1.84	1.79	1.77	1.70	1.59	1.55

(b) The stopband resonances f_{S1} and f_{S2}, caused by the periodic structure of the composite ring.

Fig. 3 shows the resonance modes of a 1-3 composite ring with $\phi = 0.88$ and $L/T = 0.57$ [6]. It is found that: f_T (=842.5 kHz), f_R (=85.75 kHz) and f_W (=341.5 kHz). Other peaks are the lateral modes f_{L1} and f_{L2}, and $3f_T$. The properties and resonance characteristics of 1-3 composite rings with various volume fractions of ceramics have been studied and results have been reported elsewhere [6].

4. Finite element model for the wirebonding transducer prototypes

Since the composite and PZT ultrasonic bonding transducers exhibit axial-symmetry about their central (z) axes, they are modeled as 360° elements with symmetry boundary conditions applied about the z axes. Fig. 4 shows schematically the 360° finite element model for these transducers. It is noted that the model is common for both transducers, since they have a similar structure. The advantage of using a full model is that all possible resonance modes including both the flexural and axial modes can be found. The material properties of PZT8 and the metal components were supplied by ASM. The loss factors were not included in the model. Linear and anisotropic properties are assumed for the piezoelectric elements while linear and isotropic properties are used for the metal components. The values of the material properties of the $\phi = 0.91$ composite necessary for the analysis have been calculated using a modified series and parallel model [1,2].

For ease of meshing, the thread of the pre-stressed screw has been ignored. Simplification has been made to the front plate and screw where the thread and threaded bore have been simplified. The ring-shaped copper electrodes are assumed to be very thin, and they have not been taken into account. All components in the assembly are assumed to have perfect mechanical coupling to each other. The h-type approach is applied to the analysis, and good convergence of the results has been reached by successively increasing the number of solid elements and hence the number of nodes so as to approximate the exact numerical solution to within 5% for frequencies up to 150 kHz. The lowest 100 natural frequencies and mode shapes of both the composite and PZT transducers have been computed using a commercial finite element software package ANSYS® version 5.6.

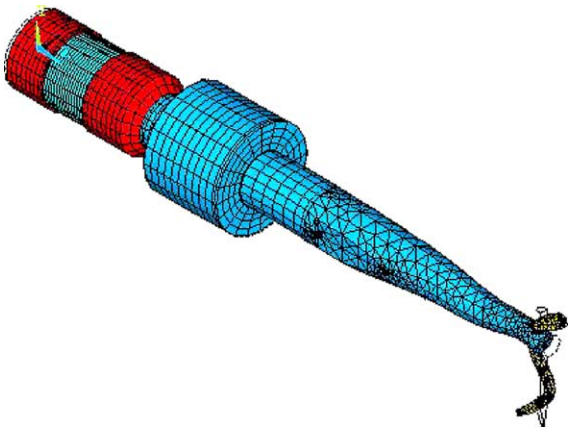

Fig. 4. Finite element model of a 64 kHz wedge wirebonding transducer shown in Fig. 2. The full model includes the wedge, barrel, and screw.

Table 2
Computed effective modes of the composite and ceramic transducers

Mode number	PZT8 ceramic		7 cpd composite		Mode shape
	f_r (kHz)	k_{eff}	f_r (kHz)	k_{eff}	
33	51.560	0.215	51.555	0.218	1λ axial mode
37	55.128	0.168	54.502	0.186	Torsional mode
38	59.146	0.144	58.735	0.144	Flexural mode
39	64.375	0.440	63.416	0.410	1.5λ axial mode
40	66.237	0.0	66.206	0.0	Torsional mode
41	66.846	0.0	66.846	0.0	Complex mode
42	68.552	0.0	67.204	0.0	Flexural mode
51	81.216	0.233	81.059	0.215	2λ axial mode

For frequencies up to 150 kHz, there are a total of 98 and 103 natural modes computed for the composite and PZT transducers, respectively. Among these modes, however, some exhibit very weak electromechanical coupling behavior ($k_{eff} < 0.05$), especially for those at higher frequencies. These modes could not be excited effectively by the electrical driving signal in practice, so they have been discarded. As a lossless system was assumed in the FEM, the actual electrical impedances cannot be determined as they have 0 Ω at the resonant frequencies and infinite ohm at the anti-resonant frequencies. Moreover, the computed k_{eff} of the composite transducer becomes larger than the real values because the losses in the planar direction of the composite ring have been neglected.

Table 2 summarizes these effective modes for the two transducers near the operating frequency. Some of the computed modes were found to be excluded by the electrical boundary conditions and are not observed in the spectrum. The computed mode shapes can be categorized as follows: axial, torsional, and complex flexural modes. The calculated axial operating frequencies, 64.375 kHz in the PZT8 ceramic transducer and 63.416 kHz in the $\phi \sim 0.91$ (7 cpd) composite transducer, are in good agreement with the measured values (64 and 62.8 kHz, from Fig. 5), and they will be discussed in the next section. From a physical standpoint, a pure axial excitation produces an axial front-to-back motion in the ultrasonic horn, which in turn, causes a large displacement at the tip of the wedge. As this motion is essentially in line with the wire to be bonded, hence the axial mode is the most desirable resonance mode. In practice, all the modes shown in Table 2 can be excited simultaneously, and the undesirable modes are difficult to

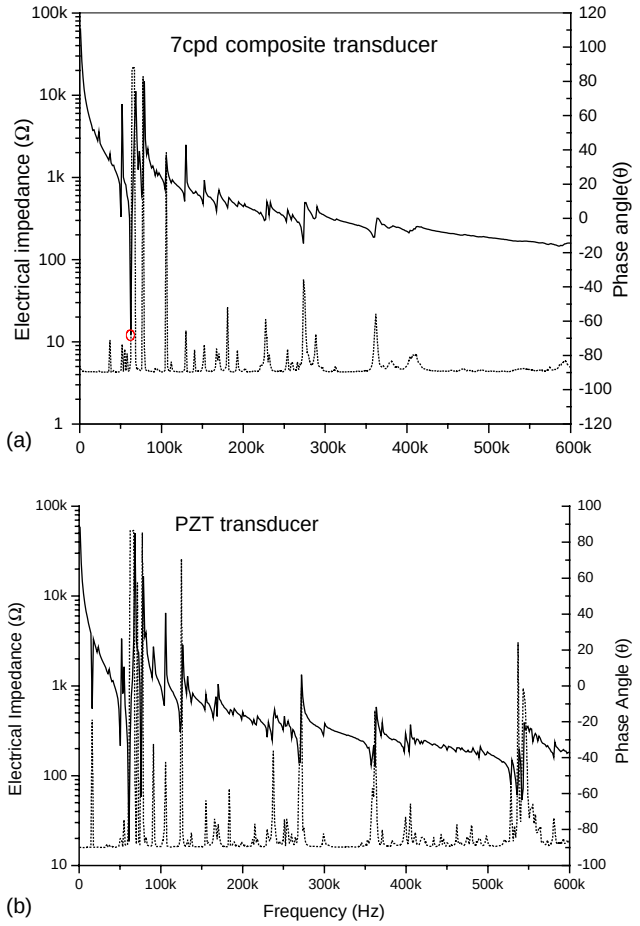

Fig. 5. Plots of electrical impedance (solid line) and phase angle (dash line) vs. frequency for the (a) $\phi = 0.91$ composite transducer, and (b) PZT transducer.

eliminate completely. This is in agreement with the experimental data shown in Fig. 5. The lateral flexural motions from side to side and the torsional motion would deteriorate the bond quality as a result of energy loss to these unwanted vibrations.

Table 2 lists the resonance modes in both the ceramic and composite transducers and their frequencies. It is seen that modes 37 and 38, the torsional and flexural modes, have large k_{eff} in both the ceramic and composite transducers. However, experimentally these two modes couple to form a complex mode with a frequency of 50.68 kHz as shown in Fig. 5. Modes 33 and 51 are found as the axial modes with different frequencies, i.e. when the length of the transducer is equal to 1 and 2 wavelengths. Their vibration profiles are quite similar to mode 39 (Fig. 4). Other torsional and complex resonances (modes 40, 41, and 42) have very small k_{eff} values and are close to zero. They are excited in the composite transducer but are farther apart than that in the ceramic transducer. The coupling factor k_{eff} and the strength of these signals has been reduced significantly in the composite transducer. By comparing the practical and simulated systems, it is found that the composite transducer can suppress the flexural mode when driven by an operating signal close to the axial mode (mode 39).

5. 1-3 Composite ultrasonic wirebonding transducer

The impedance and phase spectra of the composite and PZT transducers are shown in Fig. 5. In the PZT transducer (Fig. 5b), the strongest resonance at ~64 kHz is identified as the second axial mode, which is the designated working mode of the PZT transducer with the length of the horn and the cylindrical coupler equals to one longitudinal wavelength (the whole transducer including the driver is equal to 1.5λ). The first and third axial modes are found at 50.8 and 76.0 kHz, respectively. For frequencies ranging from 100 to 600 kHz, the PZT transducer (Fig. 5b) has very complicated resonance characteristics with many resonance peaks. In fact, when this transducer is used in bonding, the non-axial and spurious resonance modes, especially those with frequencies very close to the working axial mode or equal to its higher frequency harmonics, are likely to be excited simultaneously.

From Fig. 5a, the designated working mode of the composite transducer with 7 cpd is found at 62.8 kHz. The first and third axial modes are found at 51.2 and 76.0 kHz, respectively. No other prominent resonance is observed although some weak higher order modes can still be found in the frequency range of 150–600 kHz. The impedance spectrum is essentially pure in that the axial modes are strengthened by suppressing any non-axial and spurious modes. Some of the measured parameters of the composite transducer are listed in Table 3. The difference in the frequency of the calculated and measured thickness mode vibration f_{T} is due to the inaccuracy in the materials parameters. Also, the dimensions of the metal parts have to be adjusted in order to fine-tune the value of f_{T}. Due to the effect of polymer damping, the measured Q_{m} of the composite transducer (with $\phi = 0.91$) at the working axial mode is ~611. The PZT transducer, in contrast, has $Q_{\text{m}} \sim 1084$ which is 77% higher and thus

Table 3
Characteristics of PZT transducer and composite transducer (with composite rings of $\phi = 0.91$)

Transducer type	PZT8	$\phi = 0.91$ composite
Resonance frequency, f_{r} (kHz)	64.25	62.8
Impedance, Z_{m} (Ω)	6.69	11.35
Mechanical quality factor, Q_{m}	1084.72	611.53
Electromechanical coupling factor, k_{eff}	0.378	0.361
Average vibration amplitude at		
Horn end, front (μm)	0.788	0.788
Wedge tip, front (μm)	1.614	1.723
Wedge tip, side (μm)	0.167	0.051
F/*S* ratio	9.66	33.98
Average rise time, t_{r} (ms)	3.0	1.6
Average fall time, t_{f} (ms)	3.0	2.0
Purity by FFT (%)	90.6	94.2

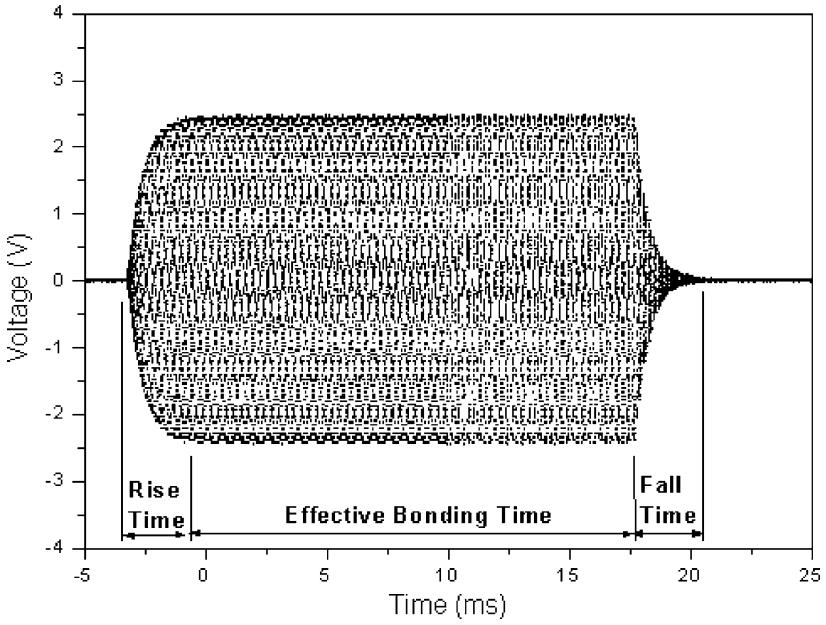

Fig. 6. Axial vibration response of the $\phi = 0.91$ composite transducer as measured at the wedge tip.

exhibiting a sharper resonance. Under a lower Q_m operation, the composite transducer will be more adaptable to various types of bonding surfaces, and can provide a reliable working platform for implementing fine-pitch bonding.

The vibration characteristics of the ultrasonic transducer were measured using a Polytec laser Doppler vibrometer connected to a digital oscilloscope (HP54522A). All transducers were affixed with the same clamping condition to the holder, and a constant input power of 0.1 W was used to drive both transducers. The waveform of the axial displacement at the end of the ultrasonic horn and at the front and side of the wedge tip were measured. By applying a fast Fourier transform (FFT) to the steady-state portion of the waveform, the corresponding displacement amplitude spectrum (in dBm) was obtained.

Table 3 shows that the longitudinal vibration displacement of the composite transducer is comparable to that of the ceramic transducer while the lateral (sideway) vibration amplitude produced by the composite transducer is about three times smaller. The F/S ratio which is the ratio of the longitudinal to lateral displacement amplitudes at the wedge tip can be used as a measure of the purity of the axial vibration. The composite transducer has a larger F/S ratio and will facilitate fine-pitch bonding. In a ceramic transducer, unwanted modes and higher harmonic vibrations are excited and the measured waveform at the wedge tip is deformed due to these complex vibrations. In a composite transducer the harmonics content of the vibration is expected to be greatly reduced. A typical axial vibration response waveform of the composite transducer is shown in Fig. 6. The composite transducer has a voltage rise and fall time ~40% shorter than that of the PZT transducer (Table 3) which indicates that it is heavily damped. This result agrees with previous findings that Q_m of the composite transducer is lower than that of the PZT transducer. Furthermore, shortening of the rise and fall time of the voltage can correspondingly increase the effective bonding time during the wire bonding process. For a constant effective bonding time, the complete bonding process can be accomplished in a shorter time if a composite transducer is used. Hence, there is an advantage in using the composite transducer in high speed bonding. Using a FFT analysis, it is seen that (Fig. 7) the excitation of other frequency components, including higher order harmonics and sub-harmonics to the fundamental, are comparatively insignificant in the composite transducer as their amplitude are about −40 dBm lower. The purity of axial excitation is ~94.2% for the composite transducer but only ~90.6% for the PZT transducer, reflecting again

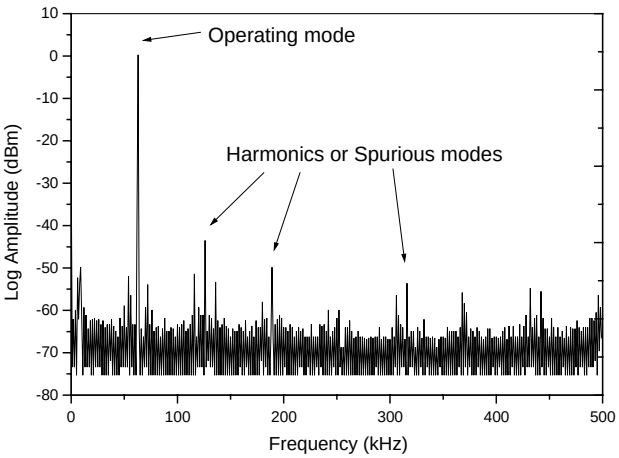

Fig. 7. Displacement amplitude spectrum (FFT) of the signal detected by the vibrometer for a $\phi = 0.91$ composite transducer.

the low mode coupling nature of the composite transducer. These observations are also in good agreement with those observed from the impedance and phase spectra.

6. Conclusion

An ultrasonic transducer for microelectronic wirebonding has been successfully fabricated using PZT/epoxy 1-3 composite rings with 81 μm epoxy width and high ($\phi = 0.91$) PZT volume fractions. Comparing to the ceramic transducer, the composite transducer has superior characteristics of low mode coupling and reduced Q_m, which make it a more efficient wirebonding transducer. Process-tests show that an ultrasonic wire bonder equipped with the composite transducer has wider operating window, purer axial vibration and reduced rise and fall time, thereby promoting the fine-pitch and high-speed capability of the bonding machine.

Acknowledgements

The authors would like to acknowledge the supports by the Center for Smart Materials of the Hong Kong Polytechnic University, the Innovation and Technology Fund (ITF UIM/29) of the HKSAR Government and ASM Assembly Automation Ltd.

References

[1] H.L.W. Chan, J. Unsworth, Simple model for piezoelectric ceramic/polymer 1-3 composites used in ultrasonic transducer application, IEEE Trans. Ultrason. Ferroelectrics Frequency Control 36 (1989) 434–441.
[2] W.A. Smith, B.A. Auld, Modeling 1-3 composite piezoelectric: thickness-mode oscillation, IEEE Trans. Ultrason. Ferroelectrics Frequency Control 38 (1991) 40–47.
[3] H. Banno, Theoretical equations for dielectric and piezoelectric properties of ferroelectric composites based on modified cubes model, Jpn. J. Appl. Phys. 24 (Suppl.) (1985) 24–32.
[4] H.L.W. Chan, I.L. Guy, Piezoelectric ceramic/polymer composites for high frequency applications, Key Eng. Mater. 92/93 (10) (1994) 275–300.
[5] S.W. Or, H.L.W. Chan, Mode coupling in lead zirconate titanate/epoxy 1-3 piezocomposite rings, J. Appl. Phys. 90 (2001) 4122–4129.
[6] C.P. Chong, H.L.W. Chan, M.H. Chan, P.C.K. Liu, Resonances in 1-3 piezocomposite rings, Appl. Phys. A, in press (published on-line 11 February 2004).
[7] S.W. Or, High Frequency Transducer for Ultrasonic Bonding, Ph.D. Thesis, The Hong Kong Polytechnic University, 2000.
[8] C.P. Chong, H.L.W. Chan, P.C.K. Liu, Vibration and resonance characteristics of PZT/epoxy 1-3 composite ultrasonic wire bonding transducers, in: Proceedings of Fourth Pacific Rim International Conference on Advanced Materials and Processing (PRICM4), vol. 2, 2001, pp. 1579–1582.
[9] H.L.W. Chan, S.W. Or, K.C. Cheng, C.L. Choy, Ultrasonic transducer, US Patent No. US 6,190,497 (20 February 2001).
[10] H.L. Li, H.L.W. Chan, C.L. Choy, Vibration characteristics of piezoceramic rings, Ferroelectrics 263 (2001) 211–216.